ICIP abu dhabi 2024

IEEE International Conference on Image Processing

27 - 30 October 2024 | Abu Dhabi, UAE

Silesian University of Technology

RESEARCH UNIVERSITY EXCELLENCE INITIATIVE

Ministry of Science and Higher Education

A NEEDLE IN A (MEDICAL) HAYSTACK: DETECTING A BIOPSY NEEDLE IN ULTRASOUND IMAGES USING VISION TRANSFORMERS

Agata M. Wijata, Bartłomiej Pyciński and Jakub Nalepa

{awijata, jnalepa}@ieee.org

October 27-30, 2024

ICIP abu dhabi 2024
IEEE International Conference on Image Processing
27 - 30 October 2024 | Abu Dhabi, UAE

Cancer statistics

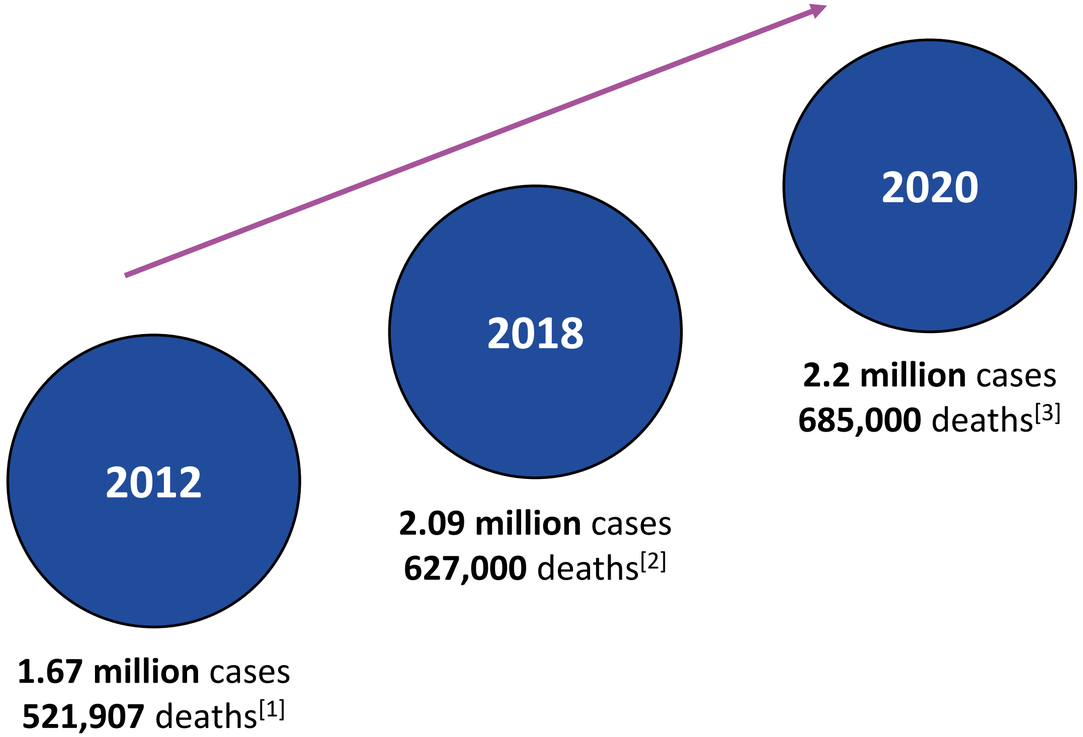

[1] WHO, Cancer Facet Sheets: Breast Cancer (2012).
[2] N. Azamjah, Y. Soltan-Zadeh, F. Zayeri, Global trend of breast cancer mortality rate: A 25-year study, Asian Pacific Journal of Cancer Prevention 20 (7) (2019) 2015–2020. doi:10.31557/APJCP.2019.20.7.2015.
[3] H. Sung, J. Ferlay, R. L. Siegel, M. Laversanne, I. Soerjomataram, A. Jemal, F. Bray, Global cancer statistics 2020: Globocan estimates of incidence and mortality worldwide for 36 cancers in 185 countries, CA: A Cancer Journal for Clinicians 71 (3) (2021) 209–249. doi:https://doi.org/10.3322/ caac.21660.

ICIP abu dhabi 2024
IEEE International Conference on Image Processing
27 - 30 October 2024 | Abu Dhabi, UAE

Breast cancer

Uncontrolled cell division of the mammary gland tissue

↓

Tumor
(malignant, benign)

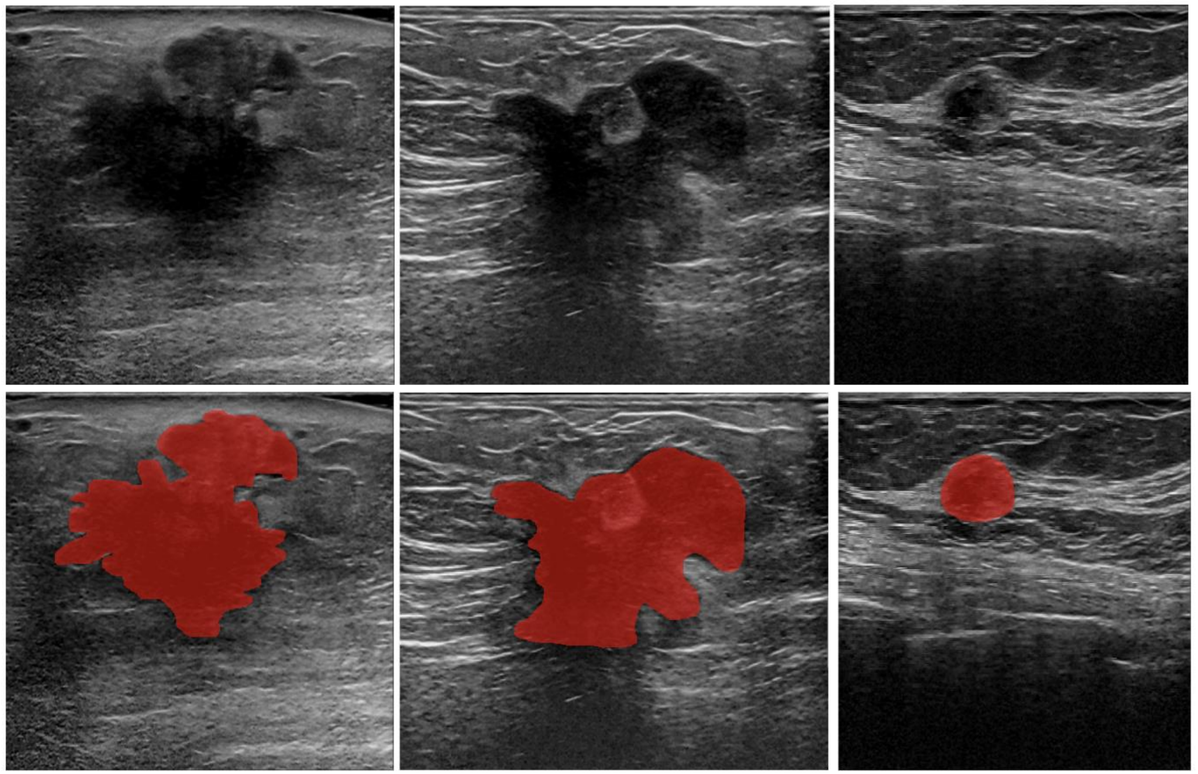

[1] V. Kumar, R. Cotran i S. L. Robbins. „Nowotwory”. In: Robbins Patologia. Wrocław: Wydawnictwo Medyczne Urban & Partner, (2005).
[2] Yap, M.H., Goyal, M., Osman, F.M., Martí, R., Denton, E., Juette, A., Zwiggelaar, R., 2019. Breast ultrasound lesions recognition: end-to-end deep learning approaches. Journal of Medical Imaging (2019).

ICIP abu dhabi 2024
IEEE International Conference on Image Processing
27 - 30 October 2024 | Abu Dhabi, UAE

Core needle biopsy (CNB)

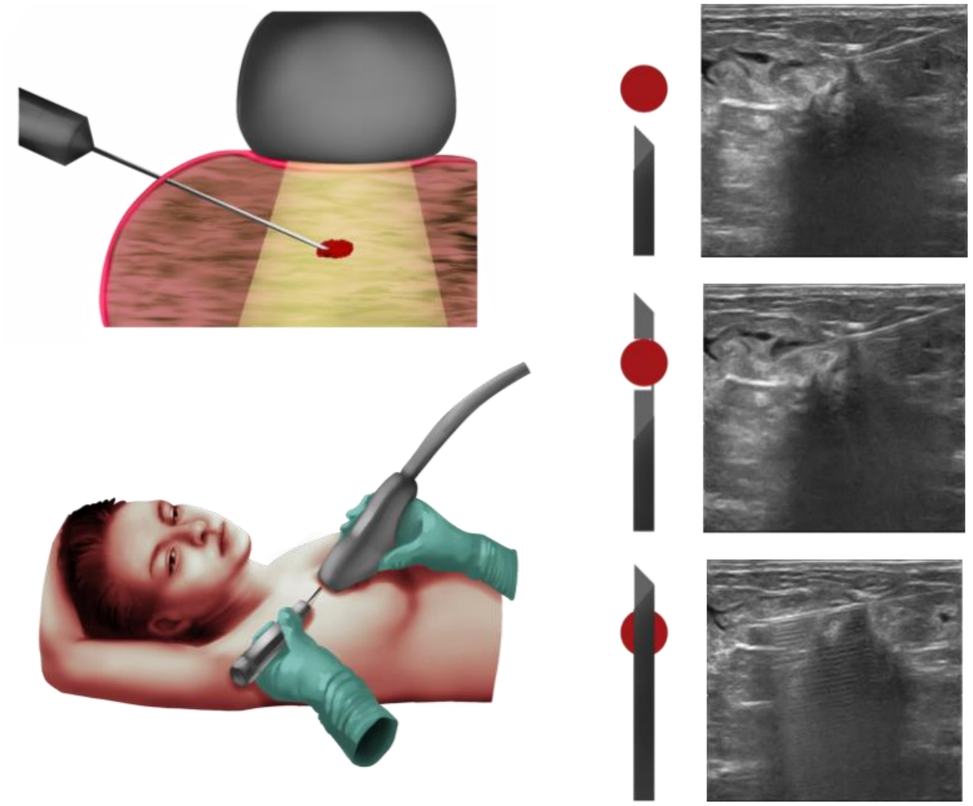

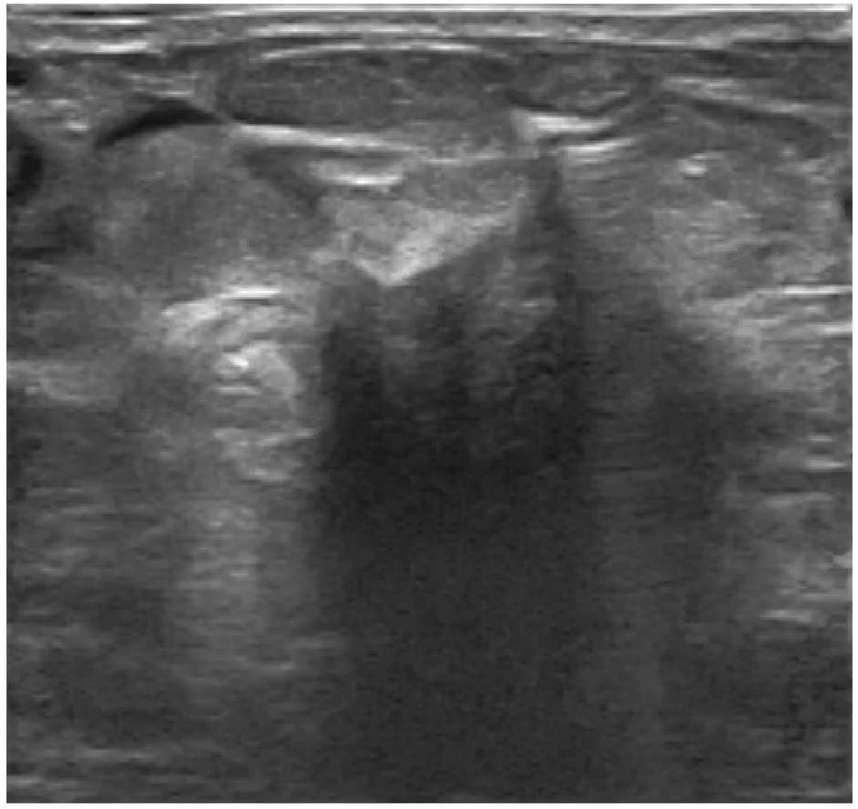

Illustration by Monika Boroń

ICIP abu dhabi 2024
IEEE International Conference on Image Processing
27 - 30 October 2024 | Abu Dhabi, UAE

Artifacts

Mirror reflection	“Comet-tail” artifact	Partially visible	
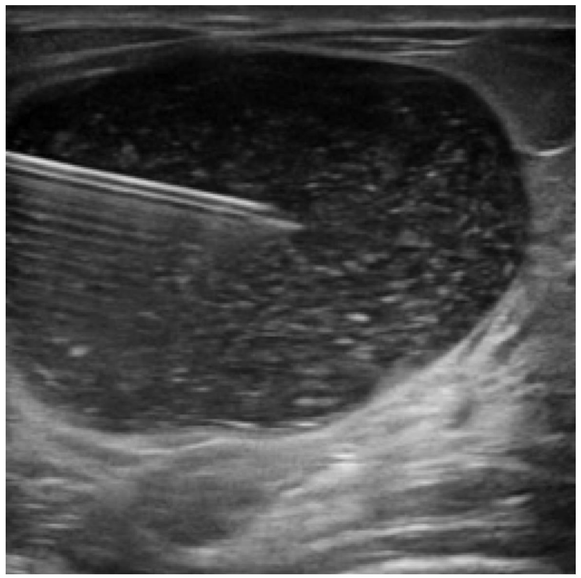	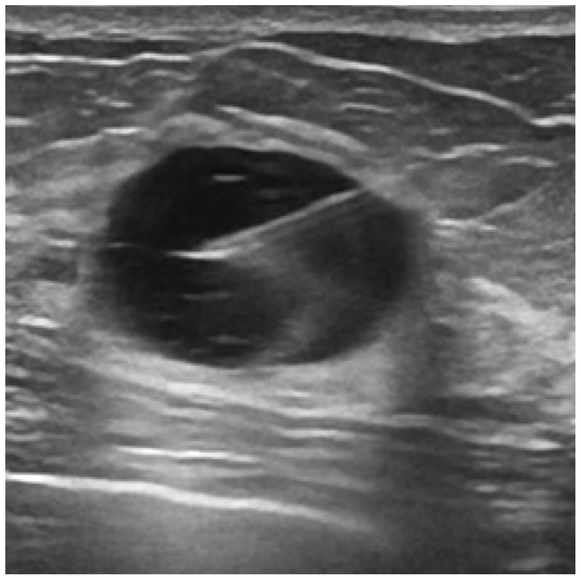	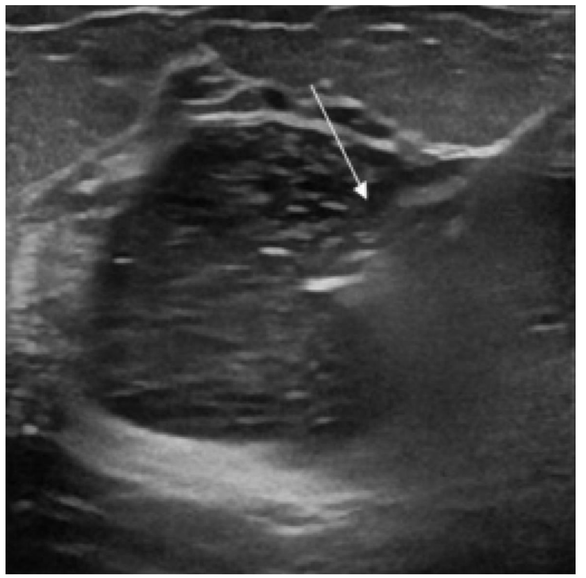	
193 pixels, 77.04°, **1.19%**	130 pixels, 70.69°, **0.34%**	221 pixels, 55.42°, **0.33%**	103 pixels, 70.91°, **0.27%**

ICIP abu dhabi 2024
IEEE International Conference on Image Processing
27 - 30 October 2024 | Abu Dhabi, UAE

State of the art

Ref.	Year	Dim.	Data acquisition	Data type	Number of set (patient)	Number of images	Data splitting	Segmentation metrics	Value	Trajectory metrics	Values
[2]	2014	3D	Sonix RP 4DC7-3/40	tissue phantom	55 sets (lamb heart)	788480	–	–	–	axis accuracy RMSE tip localization RMSE of angle α RMSE of angle β localization time	1.8 mm 1.6 mm 8° 5° 0.1 s
[3]	2015	2D	Philips CX50 L12-5	tissue phantom	1 set (pork and chicken tissue)	45	leave-one-out	–	–	$\Delta\lambda$ NLSR	0.48 mm 86.2%
				clinical data	6 patients	577				$\Delta\lambda$ NLSR	0.19 mm 99.80%
[4]	2015	2D	Philips iU22 L12-5	tissue phantom	2 sets (pork and chicken tissue)	442	–	Sen Spe	84.6% 99.0%	–	–
[5]	2017	3D	–	tissue phantom	20 set	411800	–	–	–	axis accuracy angle α angle β tip error calculation time	0.4±0.1 mm 0.0°±0.0° 0.1°±1.2° 0.6±0.3 mm 120.7±12.4 s
[6]	2018	2D	Philips iU22 C5–1	tissue phantom	1 set	60 videos	CV	–	–	success rate RMSE of angle RMSE tip localization	100% 1.28° 0.82 mm
[7]	2018	2D	Philips iU22 L12-5	tissue phantom	12 sets	364 724	a separate set (364 images)	–	–	$\Delta\theta$	2°-8°
[8]	2018	2D	Philips iU22 L12-5	tissue phantom	8 sets (porcine tissue)	ca. 1440	–	–	–	Euclidean distance	17.60±18.44 pixels
[9]	2018	3D	VL13-5 X6-1	tissue phantom	1 set (chicken and porcine tissue)	ca. 1000	five-fold CV separately for each transducer	Re Pr Spe Re Pr Spe	89.6±4.2 79.8±5.5 99.97±0.0001 87.9±4.2 83.0±3.7 99.99±0.00001	–	–
[10]	2018	2D	SonixGPS 2D C5-2/60 Clarius C3	tissue phantom	2 sets (porcine and bovine tissue)	2900	10-fold CV	–	–	$\Delta\lambda$ $\Delta\theta$	0.38±0.1 mm 0.82°±0.4°
[11]	2019	2D	SonixGPS 2D C5-2/60 Clarius C3	tissue phantom	40 video sequences 20 video sequences	12000 500	a separate set (500 images)	–	–	tip localization error processing time success rate	0.55±0.07mm 0.015 s 94%
[12]	2019	2D	Ultrasonix Sonix Touch L14-5	water phantom	3 sets	5958	a separate set	–	–	RMSE MAE	0.62 and 0.74 mm (6.08 and 7.62 pixels) 0.50±0.40 mm and 0.51±0.54 mm (4.90±3.96 and 5.24±5.52 pixels) for the axial and lateral directions
[13]	2019	2D	Vitus SIU-3	tissue phantom	1 set	ca. 160	–	–	–	RMSE	0.598 mm
[14]	2019	3D	Philips iU22 X6-1	clinical data synthetic phantom synthetic phantom	17 patients 2 sets 2 sets	149	2-fold CV	–	–	detection time position distance orientation angle	190 ms 1.59 mm 1.74 °
[15]	2020	2D	GE LOGIQ P5 GE 11L	water phantom gelatin phantom	2 sets 3 sets	8491	–	–	–	RMSE of axis localization distance	0.97 mm 1.08 mm
[16]	2020	2D	TOSHIBA VIAMO	clinical data	8 patients	996	training set (794 images), test set (202 images)	IoU DI	41.01% 56.65%	$\Delta\theta_{rms}$ $\Delta\lambda_{rms}$	13.3° 9.5 pixels
[1]	2021	2D	different sources	clinical data	91 patients	619	random 15-fold data split	F1 IoU_w Acc	0.768±0.146 0.986 ±0.006 0.992±0.004	NLSR $\Delta\lambda$ $\Delta\theta$	89.51 2.24±6.69 1.29±2.34
[17]	2021	3D	–	tissue phantom clinical data	8 sets (porcine heart) 18 patients	92 18 volumes	3-fold CV	DI DI	70.5%±9.2% 66.0%±8.3%	Hausdorff distance Hausdorff distance	7.3±4.1 voxels 8.2±2.9 voxels

Composition and size of dataset

- 15 papers used **phantom data**

The size of the phantom sets ranged from 160 to 788,480 images (mean: 101,955).

- 5 papers used **clinical data**

The size of the clinical sets ranged from 577 to 996 images (mean: 730) for 6 to 91 patients.

Cross-validation settings:

- **data sources** – 2 papers
- **data split at the set level** – 4 papers
- **data split at the patietns level** – 3 papers
- **data split at the image level** – 6 papers

Quality metrics:

- **segmentation metrics** – 5 papers
- **trajectory localization errors** – 15 papers

Image selection:

- **Image classificaition – 2**
- **Image quality – ? ?**

ICIP abu dhabi 2024
IEEE International Conference on Image Processing
27 - 30 October 2024 | Abu Dhabi, UAE

The idea

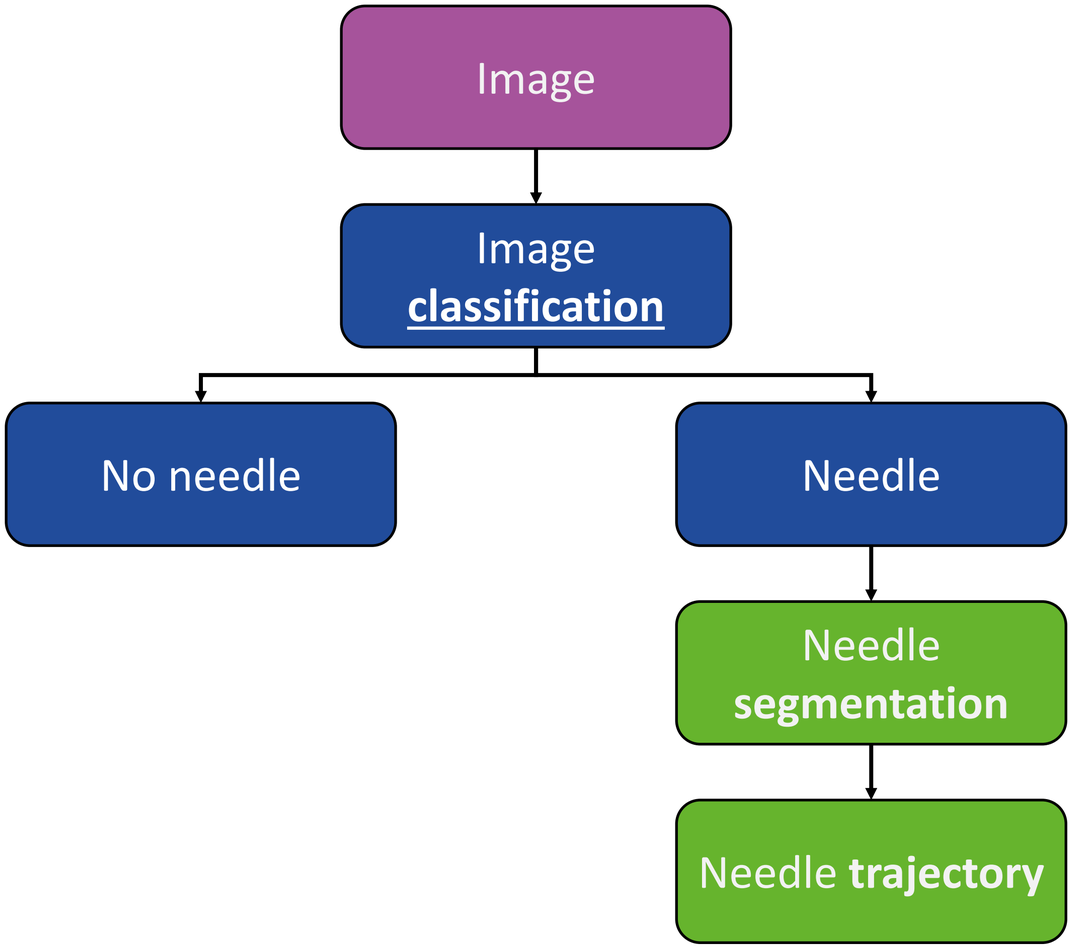

ICIP abu dhabi 2024
IEEE International Conference on Image Processing
27 - 30 October 2024 | Abu Dhabi, UAE

Flowchart

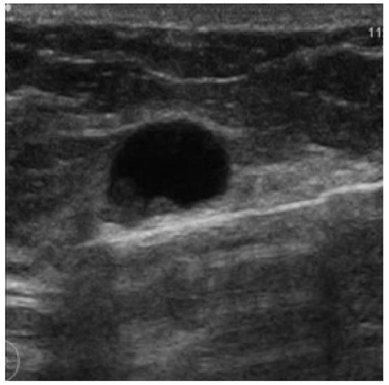

I(x,y)
384 × 384 × 3

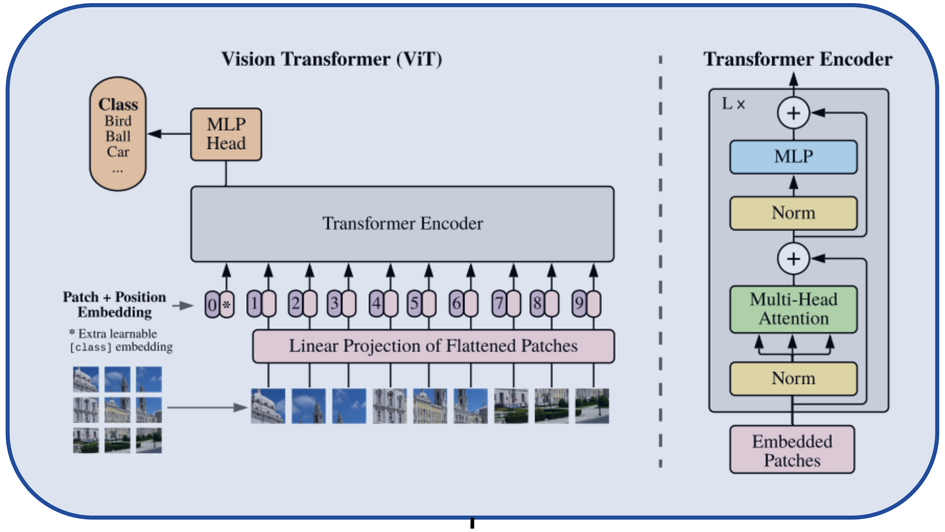

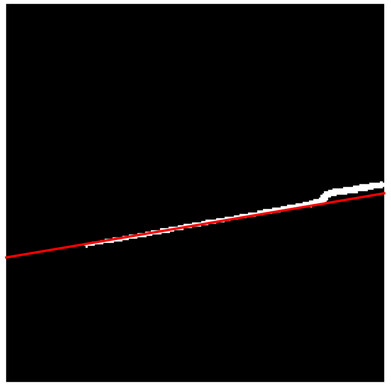

S(x,y)
384 × 384 × 1

R(x,y)
384 × 384 × 1

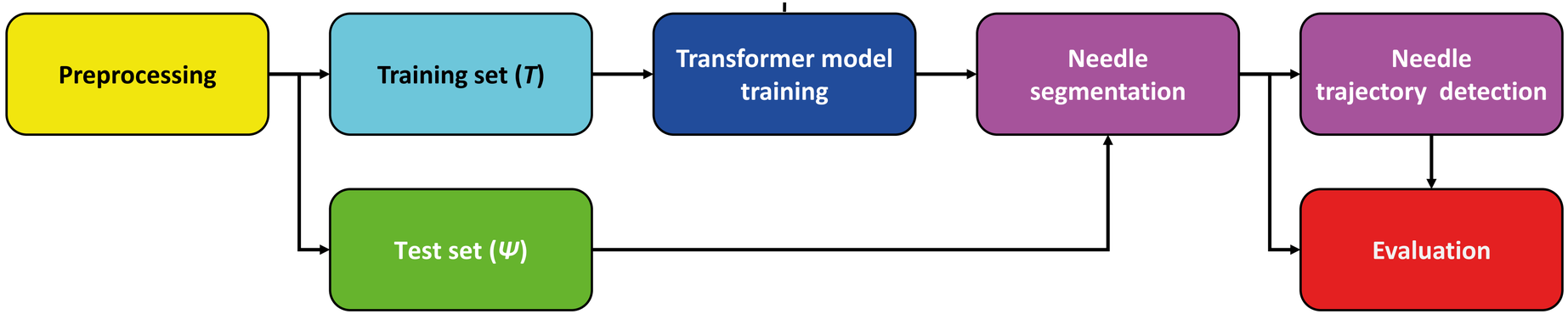

[1] A. Dosovitskiy, L. Beyer, A. Kolesnikov, D. Weissenborn,X. Zhai, T. Unterthiner, M. Dehghani, M. Minderer,G. Heigold, S. Gelly, J. Uszkoreit, and N. Houlsby, “An imageis worth 16x16 words: Transformers for image recognition atscale,” 2021.

ICIP abu dhabi 2024
IEEE International Conference on Image Processing
27 - 30 October 2024 | Abu Dhabi, UAE

Flowchart

Radon transform is applied on S(x,y)

$$R(\rho,\theta) = \int_{-\infty}^{\infty}\int_{-\infty}^{\infty} S(x,y)\delta(x\cos\theta + y\sin\theta - \rho)dxdy,$$

where ρ is the distance from the origin, θ is the angle, and δ is the Dirac delta function

Output:

- A sinogram (1D projections at different θs)
- The brightest parts – segmented objects
- Coordinates of the sinogram's maximum relate to a straight line passing through the needle: its trajectory

[1] J. Radon, "On the determination of functions from their integral values along certain manifolds," IEEE Transactions on Medical Imaging, vol. 5, no. 4, pp. 170–176, Dec 1986.

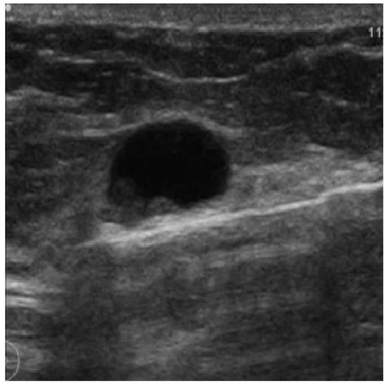

I(x,y)
384 × 384 × 3

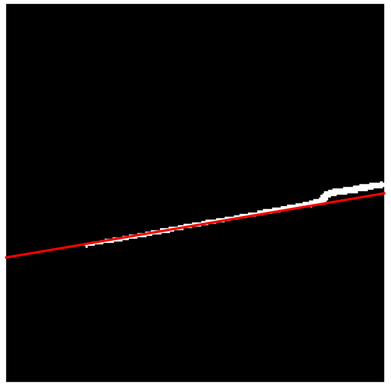

S(x,y)
384 × 384 × 1

R(x,y)
384 × 384 × 1

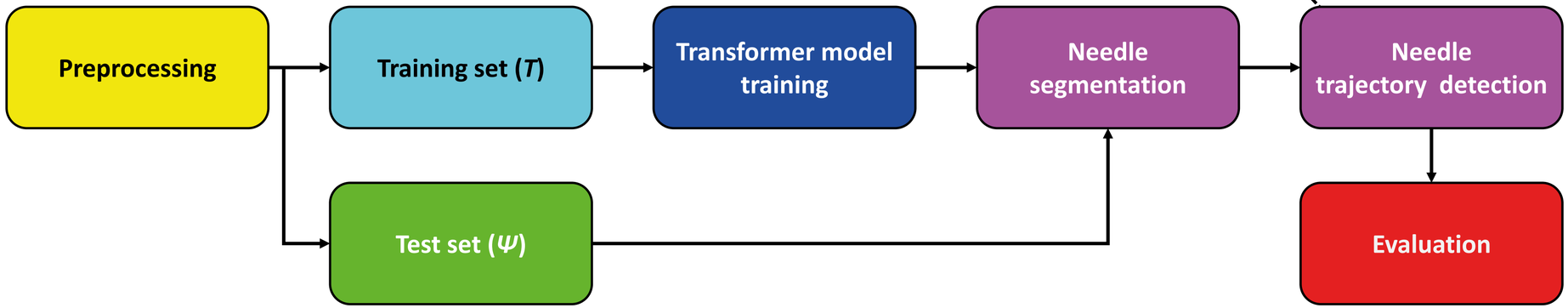

ICIP abu dhabi 2024
IEEE International Conference on Image Processing
27 - 30 October 2024 | Abu Dhabi, UAE

Dataset composition

Dataset A[1]

58 patients
(58 CNB):

- **81 2D US images with needle**
- 187 2D US images without needle

81 2D US images

Dataset B[2]

33 patients
(204 CNB):

- **538 2D US images with needle**
- 690 2D US images without needle

538 2D US images

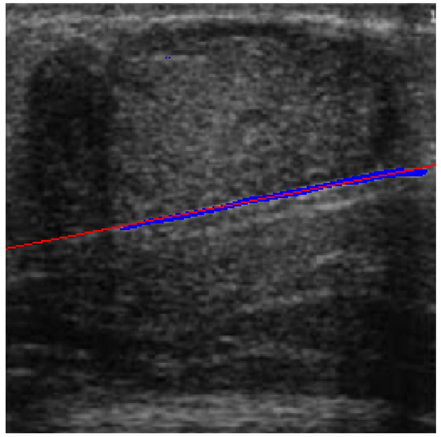

619 2D US images

[1] SonoSkills BV. Free ultrasound library offered to you by SonoSkills and Hitachi Medical Systems Europe. https://www.ultrasoundcases.info/cases/breast-and-axilla/. [accessed: June 2020]. (2020).
[2] A. Wijata, J. Andrzejewski, B. Pyciński, An automatic biopsy needle detection and segmentation on ultrasound images using a convolutional neural network, Ultrasonic Imaging 43 (5) (2021) 262–272. doi:10.1177/01617346211025267

ICIP abu dhabi 2024
IEEE International Conference on Image Processing
27 - 30 October 2024 | Abu Dhabi, UAE

Cross-Validation Scenario

ICIP2022 BORDEAUX

	(*i*)		(*ii*)		(*iii*)	
Fold↓	$\lvert \boldsymbol{T} \cup \boldsymbol{V} \rvert$	$\lvert \Psi \rvert$	$\lvert \boldsymbol{T} \cup \boldsymbol{V} \rvert$	$\lvert \Psi \rvert$	$\lvert \boldsymbol{T} \cup \boldsymbol{V} \rvert$	$\lvert \Psi \rvert$
Fold 1	(0, 33)	(58, 0)	(49, 29)	(9, 4)	(50, 29)	(8, 4)
Fold 2	—		(51, 28)	(7, 5)	(50, 29)	(8, 4)
Fold 3	—		(50, 29)	(8, 4)	(50, 29)	(8, 4)

(*i*) ***Dataset-level split*** *Test set (Ψ): Dataset A (81 images),*
Training set (T): Dataset B (538 images, with 15% random images being V)

(*ii*) ***Patient-level split*** *k-fold cross-validation*

(*iii*) ***Patient-level split*** *k-fold cross-validation (with stratification at the patient level – the ratio of patients from Dataset A and B is maintained as in (i)*

ICIP abu dhabi 2024
IEEE International Conference on Image Processing
27 - 30 October 2024 | Abu Dhabi, UAE

Evaluation metrics

Abbrev.	Ref.	Formula
Segmentation metrics		
Acc	[33]	$\mathrm{Acc} = \frac{\mathrm{TP}+\mathrm{TN}}{\mathrm{TP}+\mathrm{TN}+\mathrm{FP}+\mathrm{FN}}$
Sen	[33]	$\mathrm{Sen} = \frac{\mathrm{TP}}{\mathrm{TP}+\mathrm{FN}}$
Spe	[33]	$\mathrm{Spe} = \frac{\mathrm{TN}}{\mathrm{TN}+\mathrm{FP}}$
F1	[33]	$\mathrm{F1} = \frac{\mathrm{TP}}{\mathrm{TP}+\frac{1}{2}\cdot(\mathrm{FP}+\mathrm{FN})}$
IoU	[33]	$\mathrm{IoU} = \frac{\mathrm{TP}}{(\mathrm{TP}+\mathrm{FP}+\mathrm{FN})}$
IoU_w	[33]	$\mathrm{IoU}_w = \frac{w_{\mathrm{TP}}\cdot\mathrm{TP}}{w_{\mathrm{TP}}\cdot\mathrm{TP}+\mathrm{w}_{\mathrm{FP}}\cdot\mathrm{FP}+\mathrm{w}_{\mathrm{FN}}\cdot\mathrm{FN}}$
Trajectory localization errors		
NLSR	[22]	$\mathrm{NLSR} = \frac{1}{\mathrm{N}}\sum_{\mathrm{i}=1}^{\mathrm{N}}\mathrm{NLSR_i}$, and NLSR_i
$\Delta\lambda$	[34]	$\Delta\lambda = \lvert\lambda_{\mathrm{R_{GT}}} - \lambda_{\mathrm{R}}\rvert$
$\Delta\theta$	[34]	$\Delta\theta = \lvert\theta_{\mathrm{R_{GT}}} - \theta_{\mathrm{R}}\rvert$
$\Delta\lambda_{\mathrm{rms}}$	[24]	$\Delta\lambda_{\mathrm{rms}} = \sqrt{\frac{1}{N}\sum_{i=1}^{N}(\lambda_{\mathrm{R_{GT_i}}} - \lambda_{\mathrm{R_i}})^2}$
$\Delta\theta\mathrm{rms}$	[24]	$\Delta\theta_{\mathrm{rms}} = \sqrt{\frac{1}{N}\sum_{i=1}^{N}(\theta_{\mathrm{R_{GT_i}}} - \theta_{\mathrm{R_i}})^2}$

NLSR Needle localization success rate

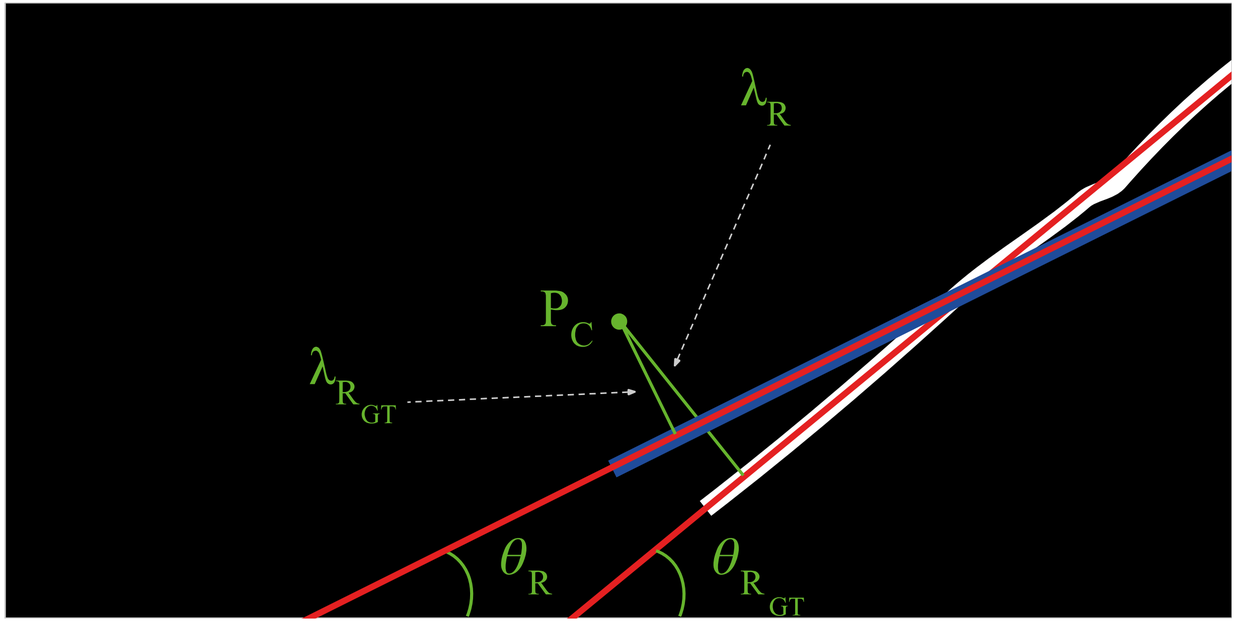

ICIP abu dhabi 2024
IEEE International Conference on Image Processing
27 - 30 October 2024 | Abu Dhabi, UAE

Results

Method	Method	Fold	Segmentation metrics						Trajectory localization errors				
			Acc	Sen	Spe	F1	IoU	IoU_w	NLSR	$\Delta\lambda$	$\Delta\theta$	$\Delta\lambda_{\text{rms}}$	$\Delta\theta_{\text{rms}}$
(i) Dataset level													
Hatt et al. [22]		*reported*[1]	—	—	—	—	—	—	99.8%	0.19 mm	—	—	—
		Dataset A	0.993	0.001	1.000	0.619	0.497	0.986	22.22%	15.19	12.73°	23.05	15.51°
Lee et al. [24]		*reported*[2]	—	—	—	0.366	0.410	—	—	—	—	9.50	13.30°
		Dataset A	0.236	0.734	0.232	0.292	0.057	0.081	58.02%	36.27	39.27°	45.81	44.48°
Wijata et al. [23]		*reported*[3]	0.742	—	—	0.768	0.655	0.986	89.5%	2.24	1.29°	9.25	3.73°
		Dataset A	0.966	0.286	0.971	0.759	0.653	0.987	85.19%	4.50	3.99°	10.13	8.81°
Ours		Dataset A	0.922	0.826	0.923	0.295	0.565	0.957	83.95%	2.33	1.18°	3.68	1.66°
(ii) Patient level													
Ours		1	0.990	0.696	0.993	0.529	0.593	0.967	96.30%	3.04	1.09	4.81	1.85
		2	0.988	0.322	0.992	0.428	0.536	0.954	79.01%	5.29	2.01	10.04	5.35
		3	0.976	0.898	0.977	0.419	0.576	0.959	95.06%	5.61	2.10	9.52	3.65
(iii) Patient level with the ratio of Dataset A and B patients maintained													
Ours		1	0.988	0.364	0.994	0.508	0.542	0.953	88.89%	2.93	0.99	4.97	1.82
		2	0.988	0.698	0.991	0.086	0.255	0.493	96.30%	2.38	0.84	3.30	1.36
		3	0.989	0.511	0.993	0.503	0.568	0.960	93.83%	4.30	1.77	8.92	3.57

[1] *Clinical*: 6 patients, 577 images, phantom (chicken and pork): 45 images. Leave one out.
[2] *Clinical*: 8 patients, 996 images. Random split: 5 patients (794 images) in $\boldsymbol{T}$, 3 (202) in Ψ.
[3] *Clinical*: 91 patients, 619 images. 15-fold CV (at the patient level) with overlaps.

ICIP abu dhabi 2024
IEEE International Conference on Image Processing
27 - 30 October 2024 | Abu Dhabi, UAE

Statistical analysis

	Hatt et al. [22]		Lee et al. [24]		Wijata et al. [23]		**Ours**	
	$\Delta\lambda$	$\Delta\theta$	$\Delta\lambda$	$\Delta\theta$	$\Delta\lambda$	$\Delta\theta$	$\Delta\lambda$	$\Delta\theta$
p	0.014	0.003	0.125	< 0.001	0.020	< 0.001	0.293	0.070
$\|r\|$	0.410	0.501	—	0.616	0.199	0.392	—	—

p *Wilcoxon test for pairs of observations*

$|r|$ *Rank correlation coefficient for matched pairs*

ICIP abu dhabi 2024
IEEE International Conference on Image Processing
27 - 30 October 2024 | Abu Dhabi, UAE

Trajectory localization errors

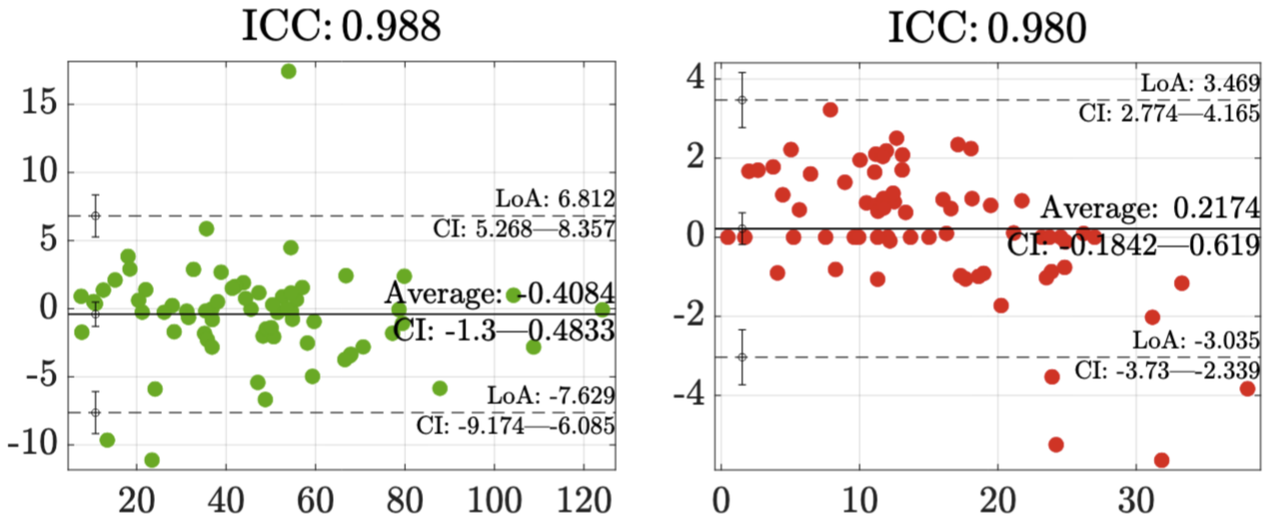

Bland-Altman plots for the Δλ and Δθ errors
ICC – Intraclass Correlation Coefficients

ICIP abu dhabi 2024
IEEE International Conference on Image Processing
27 - 30 October 2024 | Abu Dhabi, UAE

Examples

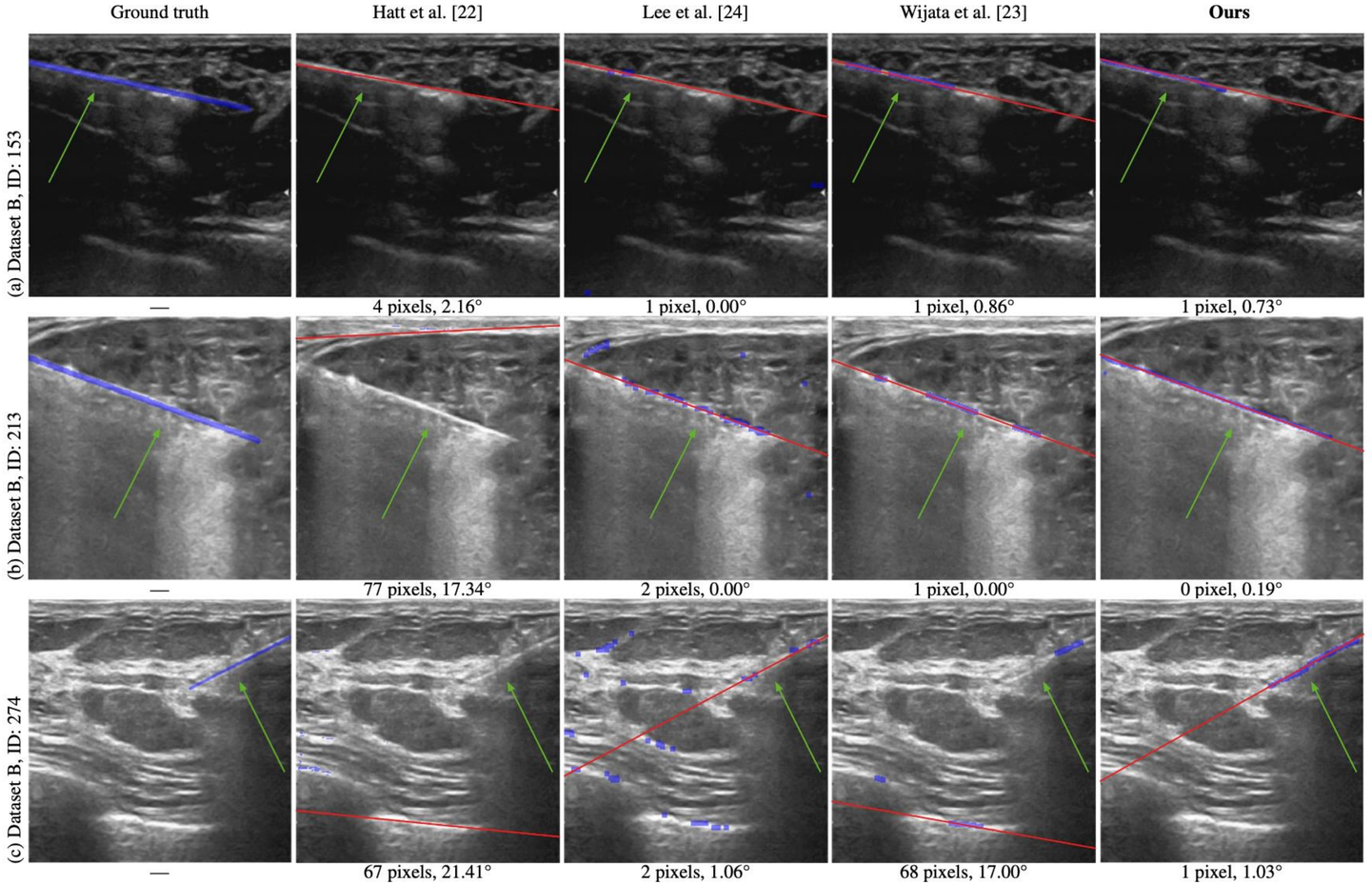

ICIP abu dhabi 2024
IEEE International Conference on Image Processing
27 - 30 October 2024 | Abu Dhabi, UAE

Conclusions

- ***Clinical significance**:* our method for detecting and tracking biopsy needles in ultrasound images **holds substantial clinical importance**, potentially **optimizing the core needle biopsy procedure**.
- ***Innovative approach**:* we introduced an **end-to-end pipeline** leveraging **Vision Transformer** for needle detection, and the **Radon transform** for trajectory determination.
- ***Experimental validation**:* **rigorous testing on two clinical ultrasound databases** demonstrated that our technique provides **superior needle segmentation and trajectory localization** compared to existing methods, while maintaining real-time performance with an **average processing time of less than 0.2 s per image**.
- ***Future implications**:* our approach represents a significant **step towards standardizing the core needle biopsy process**, addressing challenges posed by **noisy imagery**, and **reducing human bias and variability**.
- ***Potential impact**:* by enhancing the accuracy and reproducibility of needle localization, our method **could improve patient outcomes** and **procedural efficiency** in clinical settings.

ICIP abu dhabi 2024

IEEE International Conference on Image Processing

27 - 30 October 2024 | Abu Dhabi, UAE

Silesian University of Technology

RESEARCH UNIVERSITY EXCELLENCE INITIATIVE

Ministry of Science and Higher Education

A NEEDLE IN A (MEDICAL) HAYSTACK: DETECTING A BIOPSY NEEDLE IN ULTRASOUND IMAGES USING VISION TRANSFORMERS

Agata M. Wijata, Bartłomiej Pyciński and Jakub Nalepa

{awijata, jnalepa}@ieee.org

October 27-30, 2024